

Study of Different Granule Size MCM-41 Molecular Sieve as Carrier of Amoxicillin

JING-MEI LI¹, HUI YU¹, XIAO-DONG LI¹, QING-ZHOU ZHAI^{1,*} and JIAN TIAN²

¹Research Center for Nanotechnology, Changchun University of Science and Technology, Changchun 130022, P.R. China

²College of Life Science and Technology, Changchun University of Science and Technology, Changchun 130022, Jilin Province, P.R. China

*Corresponding author: Fax: +86 431 85383815; Tel: +86 431 85583118; E-mail: zhaiqingzhou@163.com; zhaiqingzhou@hotmail.com

(Received: 20 April 2011;

Accepted: 19 October 2011)

AJC-10547

In the study, two different granule size MCM-41 molecular sieves were synthesized by hydrothermal synthesis method under the different synthetical parameter. During the drug release, it is found that the drug was rapidly released from the carrier during the first 3 h. After this, the release rate became comparative lentitude. After 36 h, the release effect of the amoxicillin-(small-MCM-41) sample (SA) was 99 % and amoxicillin-(big-MCM-41) sample (BA) is 98 %. Compared SA and BA samples, the BA sample was released more rapidly in the first 3 h. However, it became more slowly after 3 h.

Key Words: MCM-41 molecular sieve, Carrier, Amoxicillin, Release.

INTRODUCTION

A series of MCM-41 mesoporous molecular sieves were synthesized successfully by Mobil in 1992¹. This material has received wide application in catalysis, adsorption separation, sensors, *etc.*, due to its high surface area, large pore volume, narrow pore size distribution and adjustable aperture²⁻⁶. Mesoporous molecular sieves were used as drug carriers, which has attracted extensive attention with further research on their structure and properties in recent years^{7,8}. These mesoporous molecular sieves with adjustable and uniform pore sizes, the rich surface silanol can be used as the new active site of the reaction with organic guest molecules⁹, so that the drug molecules bind onto the active sites with uniform distribution in the channels of mesoporous molecular sieves. That can not only slow release of the absorbed drugs, but also adjust the effect through modification (such as ion-exchange to modify adsorption ability, surface modification to enhance interaction between its surface and drugs) to achieve better effect of controlled release¹⁰. Drug slow/controlled release formulation has great significance for treatment and commercial value, which is an important research topic in modern medical technology and pharmaceutical industry. A variety of slow/controlled release drug carriers has been developed, mainly macromolecule polymer, bioglass and liposome. The advantage of mesoporous material as drug carrier is in its tunable nano-ordered pore structure and surface properties, which not only can regulate the amount of drug by adjusting the drug assembly condition (such as assembly time, concentration and the parameters of

mesoporous molecular sieves, *etc.*), but also effectively control the release rate of drug molecules by regulating of pore size, morphology, pore structure and surface properties of molecular sieves¹¹. Vallet Regi¹² for the first time reported the research on MCM-41 as drug release carrier, which soon aroused the attention of the fields in biomedicine, pharmacy and material chemistry and became research focus in the study of new drug carriers as well as a new important research topic in mesoporous materials¹³. At present, the field of molecular sieve the following areas are mainly working¹⁴ on: (1) Adjusting the physical and chemical properties of mesoporous molecular sieves such as pore size, pore volume, BET surface area, pore structure, surface modification, *etc.*⁸, (2) "Intelligent" pH value, magnetism, light, enzyme, heat, oxidation-redox controlled "induced" release¹⁵⁻¹⁸, (3) Controlled design for "molecular gate" of mesoporous molecular sieve pore¹⁹⁻²¹, (4) Study on multi-functional system of multiple drug release²², (5) Cell adhesion and biocompatibility studies, *etc.*²³. So far research on mesoporous molecular sieve as drug carrier has focused on adjusting the properties of drug release by regulating its pore size²⁴, surface properties²⁵ and morphology control²⁶ or release drug by "induction method"²⁷. Previous studies show that the morphology of molecular sieve carrier has a great impact on properties of drug release, so drug release rate can be effectively controlled by adjusting the morphology of carrier. There are specific requirements to the morphology of drug carrier used for long-circulating drug release in human body, generally particles of about 50-200 nm in diameter. The smaller nanoscale mesoporous carrier is difficult to achieve

long-term drug release because of its shorter transmission path¹⁴.

Amoxicillin is one of the most commonly used penicillin and extended spectrum β -lactam antibiotics, as a white powder, stable under acidic conditions, gastrointestinal absorption rate of 90 %. With great bactericidal effect and strong ability to penetrate the cell wall, amoxicillin is one of the more extensive oral penicillins.

In the study, two different granule size MCM-41 molecular sieves were synthesized by hydrothermal synthesis method under the different synthetical parameter and then used as the carriers of amoxicillin to investigate the effect of different particle size on the release of amoxicillin drug.

EXPERIMENTAL

Ethyl silicate (TEOS, A.R., China Medicine Group Limited Company, China); cetyltrimethylammonium bromide (CTMAB, A.R., Changzhou Xinhua Research Institute for Reagents, China); sodium hydroxide (A.R., Kaiyuan Kangyuan Chemical Reagent Factory, China); ammonia water (25 %, A.R., Beijing Chemical Reagent Factory, China); Amoxicillin (Harbin Pharmaceutical Group Co. Ltd., General Pharmaceutical Factory, China). The water for the experiment was deionized water.

The powder X-ray diffraction experiment was conducted with the D5005 model X-ray diffraction analyzer (German Siemens Company) and $\text{CuK}\alpha$ was selected as the target material. The selected wavelength of X-ray was $\lambda = 1.5418 \text{ \AA}$ and operating voltage (tube voltage) was 30 kV with operating current (tube current) of 20 mA. Fourier transform infrared spectroscopy (FT-IR) was accomplished with BRUKER Vertex-70 FTIR analyzer. KBr was used as the powder sample (the proportion of the sample was 1 wt %, KBr was 99 wt %). Pellet was used to characterize vibration situation of material's backbone structure. The low-temperature nitrogen adsorption-desorption test was conducted on the Micromeritics ASAP2010M adsorption analyzer to determine the pore structure of molecular sieves (pore size, pore volume, specific surface area, etc.) at temperature of 77 K. Before test, the samples were degassed under vacuum at 573 K for 12 h. Transmission electron micrograph (TEM) was conducted with the Jeol 2010 transmission electron microscope. Scanning electron micrograph (SEM) was measured with the Jeol JSM-5600L scanning electron microscope. A spectrophotometric method was chosen for the determination of component content of amoxicillin in the prepared host-guest composites and experiment of amoxicillin release process²⁸. A 722S spectrophotometer (Shanghai Lingguang Technique Co. Ltd., China) was used for the tests to determine component content of amoxicillin in the prepared host-guest composites and amoxicillin release process in the simulated body fluid.

Process of the experiment

Synthesis of small-MCM-41 molecular sieves: Add 1 g of CTMAB into 480 mL of deionized water at 80 °C under vigorous stirring until the solution became homogeneous. Then add 3.5 mL of 2 mol L⁻¹ NaOH solution with stirring well and 5 mL of ethyl silicate was slowly added dropwise, reacted at 80 °C for 2 h, then filtrated, washed with deionized water and

dried at room temperature to get the sample. The original sample was placed in a muffle furnace, calcined at 500 °C for 4 h to obtain small-particle MCM-41 sample²⁹.

Synthesis of big-MCM-41 molecular sieves: Add 1 g of CTMAB into 156 mL of deionized water at 80 °C under strongly stirring until the solution became homogeneous. Then add 79 mL of 25 % ammonia water with stirring well and 5 mL of TEOS was slowly added dropwise, reacted at 80 °C for 2 h, then filtrated, washed with deionized water and dried at room temperature to get the sample. The original sample was placed in a muffle furnace, calcined at 500 °C for 4 h to obtain big-particle MCM-41 sample²⁹.

Assembly of amoxicillin in MCM-41: The liquid phase method was used in this study for the assembly of amoxicillin drug into MCM-41 molecular sieves. The specific process of operation was as follows: (1) The source powder of small-MCM-41 and big-MCM-41 each 0.5 g were placed into 250 mL beakers, then 100 mL of amoxicillin methanol solution (concentration = 25 mg/mL) was added, respectively, stirred at room temperature 48 h. (2) The above mixture was filtrated, washed, dried at room temperature and put in brown bottles, respectively, stored in a dryer. The drug of small-particle MCM-41 carrier was marked as SA and big-particle MCM-41 carrier marked as BA.

Simulation experiment on amoxicillin release process: A certain amount of the prepared drug powder was soaked in 50 mL simulated body fluid (simulated body fluid, SBF)³⁰ at 37 °C with magnetic stirring. The spectrophotometric method²⁸ was used to determine the content of amoxicillin at fixed time every 1-2 h. In every process, great care must be taken to add the same amount of simulated body fluid to supplement. The simulated body fluid preparation was made by dissolving $\text{MgCl}_2 \cdot 6\text{H}_2\text{O}$ (0.305 g), 1 mol L⁻¹ HCl (40 mL), CaCl_2 (0.278 g), Na_2SO_4 (0.071 g), $\text{NH}_2\text{C}(\text{CH}_2\text{OH})_3$ (6.057 g) in distilled water in a 1000 mL volumetric flask and diluting up to the mark³¹.

RESULTS AND DISCUSSION

X-Ray diffraction analysis (XRD): Fig. 1 shows the small-angle XRD curves of prepared samples. It can be seen that both of big-MCM-41 (Fig. 1a) and small-MCM-41 (Fig. 1c) samples showed three diffraction peaks, which are (100), (110) and (200) crystal face diffraction peak. These diffraction peaks demonstrated that the prepared materials had 2D hexagonal pore structure, which was consistent with the report by the literature²⁹ and indicated that MCM-41 molecular sieves have been successfully synthesized with higher crystalline fraction. The BA (Fig. 1b) and SA (Fig. 1d) samples showed two diffraction peaks, which are (100) and (110) crystal face diffraction peak, corresponding to source powder of MCM-41 molecular sieves. That showed the decrease of crystalline degree of carriers after the assembly of amoxicillin drug into the molecular sieves of big-MCM-41 and small-MCM-41 samples. However, hexagonal pore structure was well-preserved and the prepared samples were still pore structure material.

Fig. 2 shows the wide-angle XRD curves of the prepared materials. From the figure it can be seen that each prepared sample did not appear characteristic diffraction, the source powder of amoxicillin appeared a series of diffraction peak.

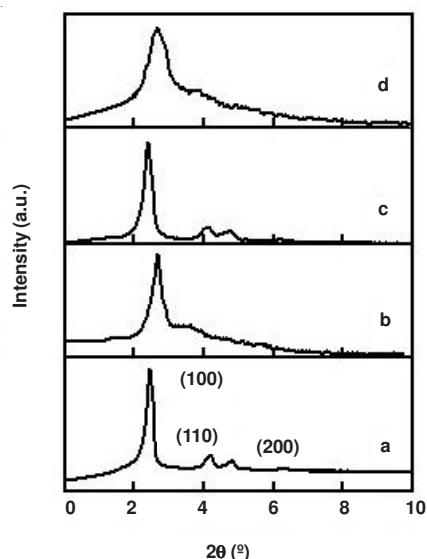


Fig. 1. Small-angle XRD patterns (a) big-MCM-41; (b) BA; (c) small-MCM-41; (d) SA

Meanwhile, BA (Fig. 2c) and SA (Fig. 2e) samples did not appear diffraction peaks of amoxicillin, which indicated that in the process of assembly, there was no amoxicillin drug gathered on the surface of molecular sieves and amoxicillin mainly distributed in the pore channels of MCM-41 molecular sieves.

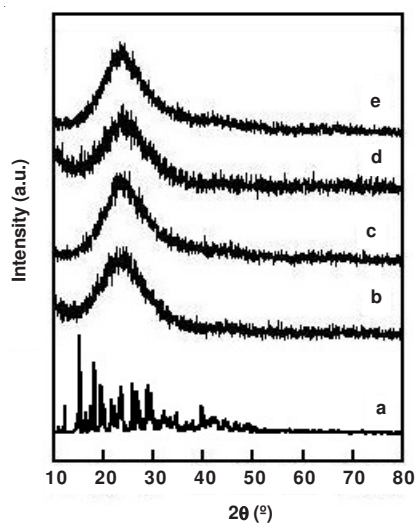


Fig. 2. Wide-angle XRD patterns a. Amoxicillin; b. big-MCM-41; c. BA; d. small-MCM-41; e. SA

Fourier transformation infrared absorption spectrum (FT-IR): Fig. 3 is the infrared spectra of prepared materials, from the figure it can be seen that in measurement range for the prepared MCM-41 molecular sieves and the drug samples which carried amoxicillin four characteristic peaks occurred. According to the order of big-MCM-41 (BA), small-MCM-41 (SA), the peaks corresponding to 471, 462, 468 and 462 cm^{-1} which can be attributed to T-O (transverse orientation) peaks were generated by bending vibrations. The peaks which located at 804, 794, 796 and 789 cm^{-1} can be attributed to the peaks generated by Si-O-Si of TO_4 symmetric stretching vibration. The peaks which located at 966, 968, 968, 964 cm^{-1} and

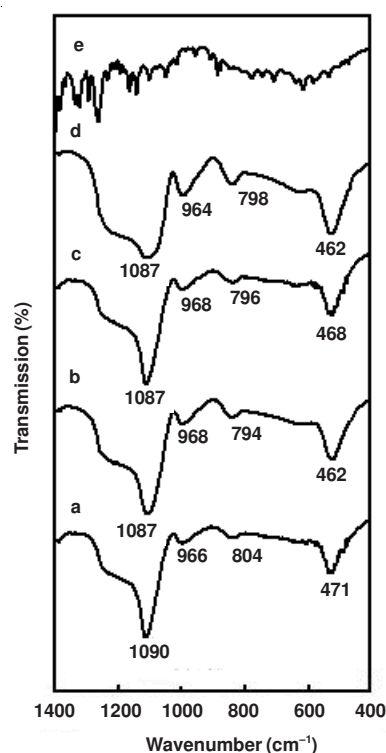


Fig. 3. FT-Infrared spectra of each sample a. big-MCM-41; b. BA; c. small-MCM-41; d. SA; e. amoxicillin

at 1090, 1087, 1087, 1087 cm^{-1} can be attributed to the peaks generated by Si-O-Si of TO_4 asymmetric stretching vibration³². The existence of these characteristic peaks may prove the existence of MCM-41 skeleton. Besides, the peaks which located at 966, 968, 968, 964 cm^{-1} can also be attributed to the ones generated by Si-OH non-bridging oxygen atoms' stretching vibration.

Compared the infrared absorption spectra of sample BA (Fig. 3b) and sample SA (Fig. 3d) with the source powder of amoxicillin, there were not obvious amoxicillin characteristic absorption peak in measurement range. Their infrared absorption spectra and the corresponding MCM-41 molecular sieve source powder were basically consistent. This phenomenon showed that after MCM-41 molecular sieve loaded with amoxicillin, the prepared drug was still pore structure material with well-preserved skeleton of molecular sieve and also indicated that no gathered guest material distributed on outer surface of the carrier. Amoxicillin was mainly distributed in molecular sieve's pore channels, which was consistent with the results of XRD.

Analysis of nitrogen adsorption and desorption: Fig. 4 refers to the nitrogen adsorption and desorption isotherms of prepared materials. From this figure we can see that nitrogen adsorption and desorption isotherms were IV-shape and they had a clear adsorption and desorption branching. Big-MCM-41 in the scope of $0.52 \geq P/P_0 \geq 0.35$ and small-MCM-41 in the scope of $0.52 \geq P/P_0 \geq 0.29$, the adsorption branching and reconciliation adsorption branching jumped suddenly and turned up a H1-shape hysteresis loop. This was mainly because N_2 's absorption in molecular sieve pore channels was unilayer at the very beginning and this procedure was reversible, the

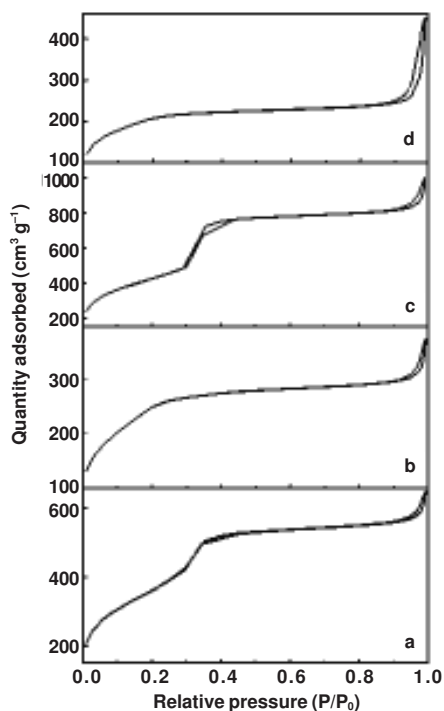


Fig. 4. Adsorption-desorption isotherms a. big-MCM-41; b. BA; c. small-MCM-41; d. SA

adsorption branching and reconciliation adsorption branching didn't jump and there was not hysteresis loop. But when the relative and differential pressure increased to a certain degree, phenomenon of capillary condensation would occurred, then the adsorption branching and reconciliation adsorption branching jumped and hysteresis accordingly. For big-MCM-41 in the scope of $0.99 \geq P/P_0 \geq 0.92$ and small-MCM-41 in the scope of $0.99 \geq P/P_0 \geq 0.94$, for the adsorption branching and reconciliation adsorption branching the second jump occurred. At the same time, there was also a hysteresis phenomenon. This is because the microbore formed between molecular sieves pellet, when the relative and differential pressure reached a certain degree, there will be the second phenomenon of capillary condensation. In the case of sample BA and SA, the drugs were assembled into molecular sieves channels which resulted in aperture reduction greatly (Fig. 5). Generally speaking, differential pressure of phenomenon of capillary condensation was related to aperture size. The bigger of the aperture, the bigger of differential pressure of the capillary condensation. Therefore, the differential pressure of sample BA and SA was very small when phenomenon of capillary condensation occurred. But adsorption and desorption isotherms were still IV-shape. Prepared samples kept the mesoporous channels structure.

The specific surface area was calculated by BET (Brunner-Emmett-Teller)³³ and the distribution of aperture size was calculated by BJH (Barrett-Joyner-Halenda)³⁴. The correlation data involved in each parameter's calculation were based on the adsorption branching of nitrogen adsorption and desorption isothermal line (Table-1). From these data we can find that comparing sample BA and SA with the corresponding samples of big-MCM-41 and small-MCM-41, the specific surface area, pore volume and aperture were greatly reduced and this was mainly because the guest materials entered the subject pore channels. From this, it is concluded that the guest materials of amoxicillin had already entered into pore channels.

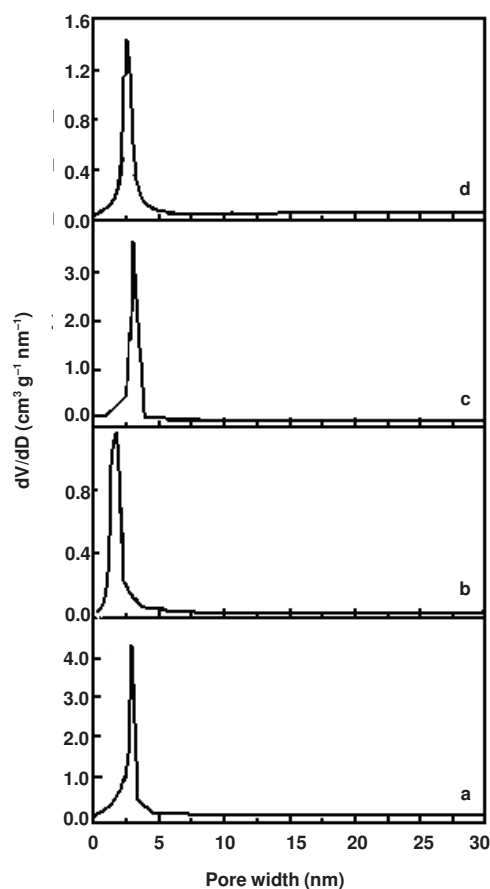


Fig. 5. Pore size distribution patterns a. big-MCM-41; b. BA; c. small-MCM-41; d. SA

Scanning electron micrograph (SEM): Fig. 6 refers to the scanning electron micrographs of prepared materials. From the pictures it is seen that the prepared samples like big-MCM-41, BA, small-MCM-41, SA were all micro sphere. Through

TABLE-1
PORE STRUCTURE PARAMETERS OF SAMPLES

Sample	d_{100} (nm)	a_0^a (nm)	BET surface area (m^2/g)	Pore volume ^b (cm^3/g)	Pore size ^c (nm)
Big-MCM-41	3.60	4.16	1308.1	0.961	3.27
BA	3.21	3.71	845.8	0.416	2.31
Small-MCM-41	3.34	3.85	1329.1	1.331	3.55
SA	3.33	3.85	675.4	0.508	2.82

^a $a_0 = \frac{2}{\sqrt{3}}d_{100}$. ^bBJH adsorption cumulative volume of pores. ^cPore size calculated from the adsorption branch.

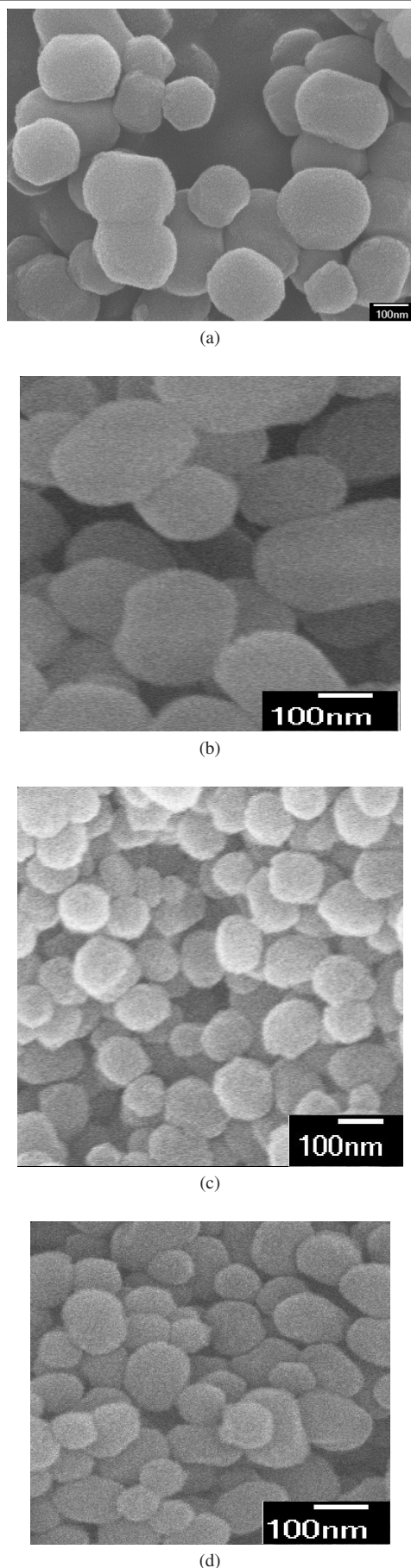


Fig. 6. SEM image of the samples a. big-MCM-41; b. BA; c. small-MCM-41; d. SA

the calculation, the average diameter of sample big-MCM-41 was 267 nm, the average diameter of sample BA was 260 nm, the average diameter of sample small-MCM-41 was 125 nm and the average diameter of sample SA was 118 nm.

Transmission electron micrograph (TEM): Fig. 7 shows the transmission electron micrograph of each samples. Picture a was taken with the beam direction perpendicular to the pores and picture b was taken with the beam direction parallel to the pores. From the transmission electron micrograph, each sample synthesized in present work, was with the beam direction perpendicular to the pores had highly ordered pore structures and the sample which was with the beam direction parallel to the pores showed regular lattice construction images. From these transmission electron micrograph, it is observed that the samples had mesopore pore channel structure of two dimensional planar hexagon. After assembling guest materials of amoxicillin in molecular sieve pore, the mesopore pore channel of molecular sieve planar hexagon had been preserved, so the existence of agminate pellets of guest materials from the picture is not observed.

Release curve of amoxicillin: The measurement of amoxicillin assembly quantity: At first, the concentration of alcoholic solution of amoxicillin which before assembled was measured by literature method²⁸ and calculated the amoxicillin quality of the solution; then measured the concentration of amoxicillin methanol solution which was adsorped by MCM-41 molecular sieve, the volume of solution and calculate amoxicillin quality of the solution in the same way; finally, according to the difference of amoxicillin quality that measured in the two times to calculate amoxicillin quantity of the assembly molecular sieve and calculate the quality percentage of prepared amoxicillin in the study. According to this method, the content of sample SA was 16 % and the content of sample BA was 14 %.

Drug releasing: Fig. 8 shows the release curve of amoxicillin in simulated body fluid. From the curve, it is found that the drug was rapidly released from the carrier in first 3 h. The release rate of sample (SA) was 51 % at 5 h, while the release rate of sample (BA) was 53 % at 4 h. This is because the drug distributed on the surface and nearby the pore of MCM-41 was contacted with the body fluid directly and rapidly released. After that because the hole block was getting bigger and bigger when the body fluid entered into the carrier pore and the release rate became comparative lentitude. For the sample (SA), the release rate was 99 % after 36 h; for the sample (BA), it was 98 % after 36 h. Compared the release process of sample (SA) with sample (BA), it was found that the release rate of sample (BA) was much quicker during the first 3 h, specific surface area were much bigger (Fig. 1). In the release process, the carriers were well contacted with body fluid which resulted in that release rate was much quicker in this stage. Because of the small mesoporous aperture, big pellet and long pore channel. (Fig. 6), the hole resistance was much larger and release rate became much smaller in the further release.

Conclusion

In this study, two different granule size MCM-41 molecular sieve were synthesized by hydrothermal method. Assembled

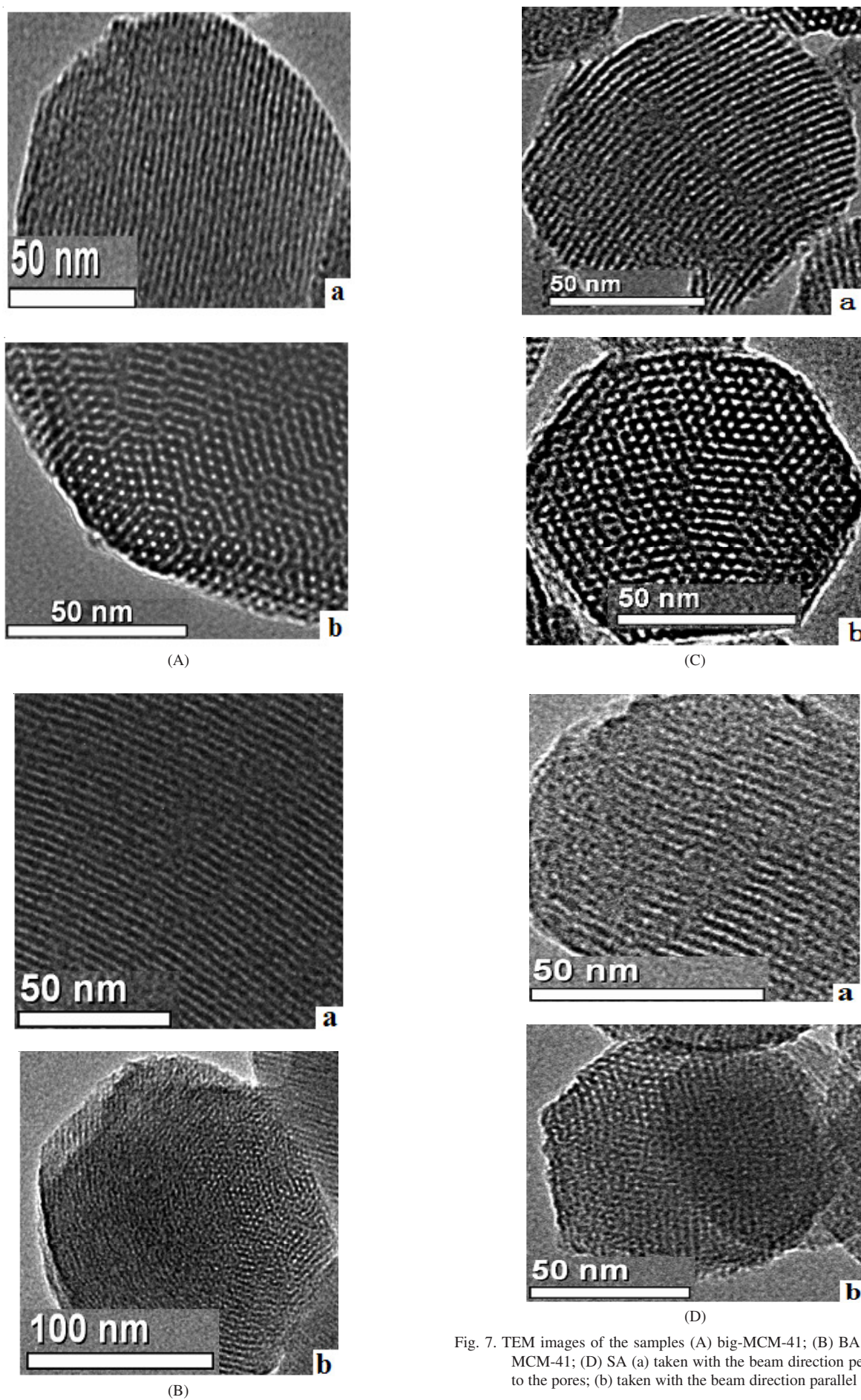


Fig. 7. TEM images of the samples (A) big-MCM-41; (B) BA; (C) small-MCM-41; (D) SA (a) taken with the beam direction perpendicular to the pores; (b) taken with the beam direction parallel to the pores

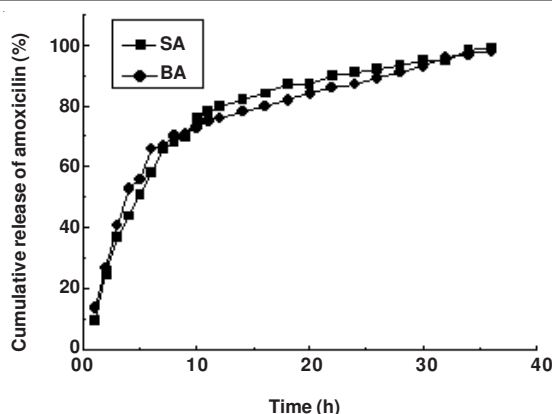


Fig. 8. Amoxicillin release profile in a simulated body fluid

the amoxicillin to molecular sieves pore by liquid-phase grafting method and served as the carriers amoxicillin drug, it was used to follow-up the release processes of prepared drugs in the simulated body fluid. Through a series of characterization, it was found that liquid-phase grafting method could assembled amoxicillin into MCM-41 molecular sieve pore channels successfully and the drugs kept the features of mesoporous pore. Through the simulated release process, we found that the drug was rapidly released from the carrier in the 3 h. The release effect of sample (SA) was 51 % after 5 h and the release effect of sample (BA) was 53 % at 4 h. After this, the release rate became comparative lentitude. After 36 h of release, the release effect of the amoxicillin-(small-MCM-41) sample (SA) was 99 % and amoxicillin-(big-MCM-41) sample (BA) was 98 %. On comparing SA and BA samples, the BA sample was released more rapidly in the first 3 h. However, it became more slowly after 3 h. MCM-41 molecular sieves can be served as the carriers of drugs, then it may greatly reduce the release rate of drugs, plays a role in slow release and enhances the drug effect and the use factor.

ACKNOWLEDGEMENTS

The authors are grateful to the financial support from Department of Education of Jilin Province, P. R. China. The grant number was 2010JYT10, KYC-JC-XM-2010-014.

REFERENCES

- J.S. Beck, J.C. Vartuli, W.J. Roth, M.E. Leonowicz, C.T. Kresge, K.D. Schmitt, C.T. Chu, D.H. Olson, E.W. Sheppard, S.B. McCullen, J.B. Higgins and J.L. Schlenker, *J. Am. Chem. Soc.*, **114**, 10834 (1992).
- N.Y. Yu, Y.J. Gng, S.G. Wang, D. Wu, Y.H. Sun, Q. Luo, W.Y. Liu and F. Deng, *Acta Chim. Sin.*, **61**, 58 (2003).
- J.W. Zhao, F. Gao, Y.L. Fu, W. Jin, P.Y. Yang and D.Y. Zhao, *Chem. Commun.*, **7**, 752 (2002).
- X. Yuan, Y.Y. Liu, S.P. Zhuo, W. Xing, Y.Q. Sun, X.D. Dai, X.M. Liu and Z.F. Yan, *Acta Chim. Sin.*, **65**, 1814 (2007).
- J.H. Zhu, W. Shen, H.L. Xu, Y.M. Zhou, C.Z. Yu and D.Y. Zhao, *Acta Chim. Sin.*, **61**, 202 (2003).
- W.J. Xu, Q. Gao, Y.P. Xu, D. Wu and Y.H. Sun, *Acta Chim. Sin.*, **66**, 1658 (2008).
- C.Y. Lai, B.G. Trewyn, D.M. Jeftinija, K. Jeftinija, S. Xu, S. Jeftinija and V.S. Lin, *J. Am. Chem. Soc.*, **125**, 4451 (2003).
- B. Munoz, A. Ramila, J. Perez-Pariente, I. Diaz and M. Vallet-Regf, *Chem. Mater.*, **15**, 500 (2003).
- A. Ramila, B. Munoz, J. Perez-Pariente and M. Vallet-Regf, *J. Sol-Gel Sci. Technol.*, **26**, 1199 (2003).
- L. Gao and J.H. Sun, *Acta Petrol. Sin.*, **24**, 265 (2006).
- F.Y. Qu, L.F. Cui, S.Y. Huang and G.S. Zhu, *Chem. J. Chin. Univ.*, **28**, 1440 (2007).
- M. Vallet-Regf, A. Ramila, R.P. Del-Real and J. Perez-Pariente, *Chem. Mater.*, **13**, 308 (2001).
- P.P. Yang, S.S. Huang, D.Y. Kong, J. Lin and H.G. Fu, *Inorg. Chem.*, **46**, 3203 (2007).
- Y.P. Xu, Y. Wang, F.Y. Qu, X. Wu and J.Y. Ma, *J. Ceram.*, **31**, 5 (2010).
- N.K. Mal, M. Fujiwara and Y. Tanaka, *Nature*, **421**, 353 (2003).
- S.H. Hu, T.Y. Liu, H.Y. Huang, D.M. Liu and S.Y. Chen, *Langmuir*, **24**, 239 (2008).
- G. Han, C. You, B. Kim, R.S. Turingan, N.S. Foes, C.T. Martin and V.M. Rotello, *Angew. Chem. Int. Ed.*, **45**, 3165 (2006).
- C.Y. Park, K. Kee and C.H. Kim, *Angew. Chem. Int. Ed.*, **48**, 127 (2009).
- S. Angelos, Y.W. Yang, K. Patel, J.F. Stoddart and J.I. Zink, *Angew. Chem. Int. Ed.*, **47**, 2222 (2008).
- E. Aznar, D. Marcos, R. Martinez-Manez, F. Sancenon, J. Soto, P. Amoros and C. Guillem, *J. Am. Soc. Chem.*, **131**, 6833 (2009).
- S.S. Agasti, A. Chompoosor and C.C. You, *J. Am. Soc. Chem.*, **131**, 5728 (2009).
- Y.F. Zhu and S. Kaskel, *Micropor. Mesopor. Mater.*, **118**, 176 (2009).
- X. Li, X.P. Wang, L.X. Zhang, H.R. Chen and J.L. Shi, *J. Biomed. Mater. Res. A-Appl. Biomater.*, **89B**, 148 (2009).
- J. Andersson, J. Rosenholm, S. Areva and M.M. Linden, *Chem. Mater.*, **16**, 4160 (2004).
- F.Y. Qu, G.S. Zhu, S.Y. Hung, S.G. Li and S.L. Qiu, *Chem. Phys. Chem.*, **7**, 400 (2006).
- F.Y. Qu, G.S. Zhu, S.Y. Hung, S.G. Li, J.Y. Sun, D.L. Zhang and S.L. Qiu, *Micropor. Mesopor. Mater.*, **92**, 1 (2006).
- Y.F. Zhu, J.L. Shi, W.H. Shen, X.P. Dong, J.W. Feng, M.L. Ruan and Y.S. Li, *Angew. Chem. Int. Ed.*, **44**, 5083 (2005).
- H.B. Lu, H. Li and L.Z. Yang, *Sichuan Med. J.*, **21**, 344 (2000).
- Q. Cai, Z.S. Luo, W.Q. Pang, Y.W. Fan, X.H. Chen and F.Z. Cui, *Chem. Mater.*, **13**, 258 (2001).
- T. Kokubo, H. Kushitani and S. Sakka, *J. Biomed. Mater. Res.*, **24**, 721 (1990).
- P. Horcajada, A. Ramila, J. Perez-Pariente and M. Vallet-Reg, *Micropor. Mesopor. Mater.*, **68**, 105 (2004).
- S.Y. Yu, L.P. Wang and B. Chen, *Chem. Eur. J.*, **11**, 3894 (2005).
- S. Brunauer, P.-H. Emmett and E. Teller, *J. Am. Chem. Soc.*, **60**, 309 (1938).
- E.P. Barrett, L.G. Joyner and P.P. Halenda, *J. Am. Chem. Soc.*, **73**, 373 (1951).